ORIGINAL ARTICLE

Supporting Information: The Conformational Space of a Flexible Amino Acid at Metallic Surfaces

Dmitrii Maksimov[1,2] | **Carsten Baldauf**[1] | **Mariana Rossi**[1,2]

1 | DETAILS OF THE CALCULATIONS

For Cu, Ag and Au, the bulk lattice constants were determined by optimizing the fcc unit cell. The convergence criteria were set to 0.001 eV/Å for the final forces, 10^{-4} e/Bohr^3 for the charge density, and 10^{-5} eV for the total energy of the system. A 30×30×30 k-grid mesh was used for the sampling of the Brillouin zone. Relativistic effects were considered by the zeroth order regular approximation (ZORA) [1, 2]. The values obtained with the PBE functional[3] are in good agreement with previous works [4, 5] and are shown in Table S1. In that Table, we compare these values with lattice constants obtained when including pairwise van der Waals dispersion from the original Tkatchenko-Scheffler scheme (+vdW)[6] and from the one that includes an effective electronic screening optimized for metallic surfaces (+vdW^{surf})[7][1].

TABLE S1 Lattice constants (in Å) of bulk metals determined with the PBE, PBE+vdW and PBE+vdW^{surf} functionals (*light* settings).

Method	Cu	Ag	Au
PBE	3.633	4.156	4.157
PBE+vdW	3.545	4.077	4.114
PBE+vdW^{surf}	3.604	4.022	4.173
Exp	3.603	4.069	4.065

[1] We here used the original parameters published in Ref. [7].

TABLE S2 Fermi energies calculated with the PBE functional for the 4-layer slabs with (111) surface orientation used in our calculations of the binding energies of Arg-H^+ to the different surfaces. All values in eV.

	Cu	Ag	Au
Slab E_f	-4.73	-4.30	-5.02

TABLE S3 Relative binding energies (in eV) of relaxed Arg@Cu for different surface unit cell sizes with a 8×8×1 k-grid for the cell sizes less than 10×12 and 4×4×1 for the 10×12 unit cell. All numbers are reported with respect to the binding energy for the structure A modelled with a 5×6 surface unit cell.

size	A	B	C
5×6	0.000	0.011	0.216
6×6	-0.011	-0.013	0.190
6×7	-0.021	-0.030	0.174
10×12	-0.048	-0.053	0.151

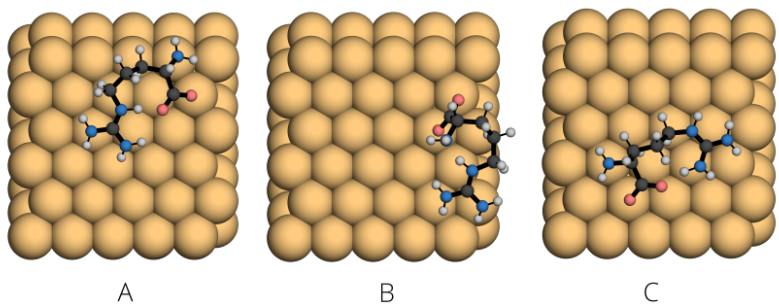

FIGURE S1 Structures that were used for the surface unit cell size convergence test of Arg@Cu. Image unit cell size is 5×6.

TABLE S4 Relative binding energies (in eV) of relaxed Arg-H^+@Cu for different surface unit cell sizes with a 8×8×1 k-grid for the cell sizes less than 10×12 and 4×4×1 for the 10×12 unit cell. All numbers are reported with respect to the binding energy for the structure A modelled with a 5×6 surface unit cell.

size	A	B	C
5×6	0.000	0.080	0.035
6×6	-0.050	0.041	-0.017
6×7	-0.055	0.029	-0.033
10×12	-0.044	-0.007	-0.057

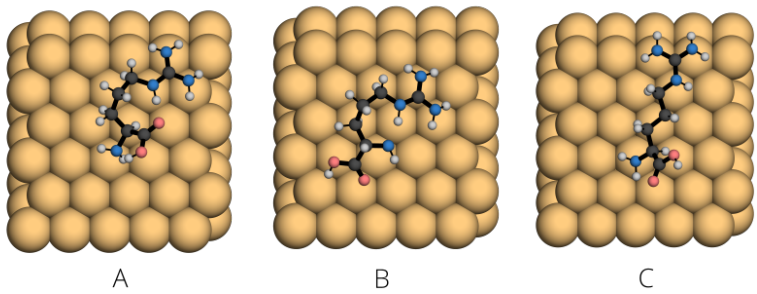

FIGURE S2 Structures that were used for surface unit cell size convergence test for Arg-H^+@Cu. Image unit cell size is 5×6.

2 | FAMILY CLASSIFICATION ACCORDING TO HYDROGEN BOND PATTERNS

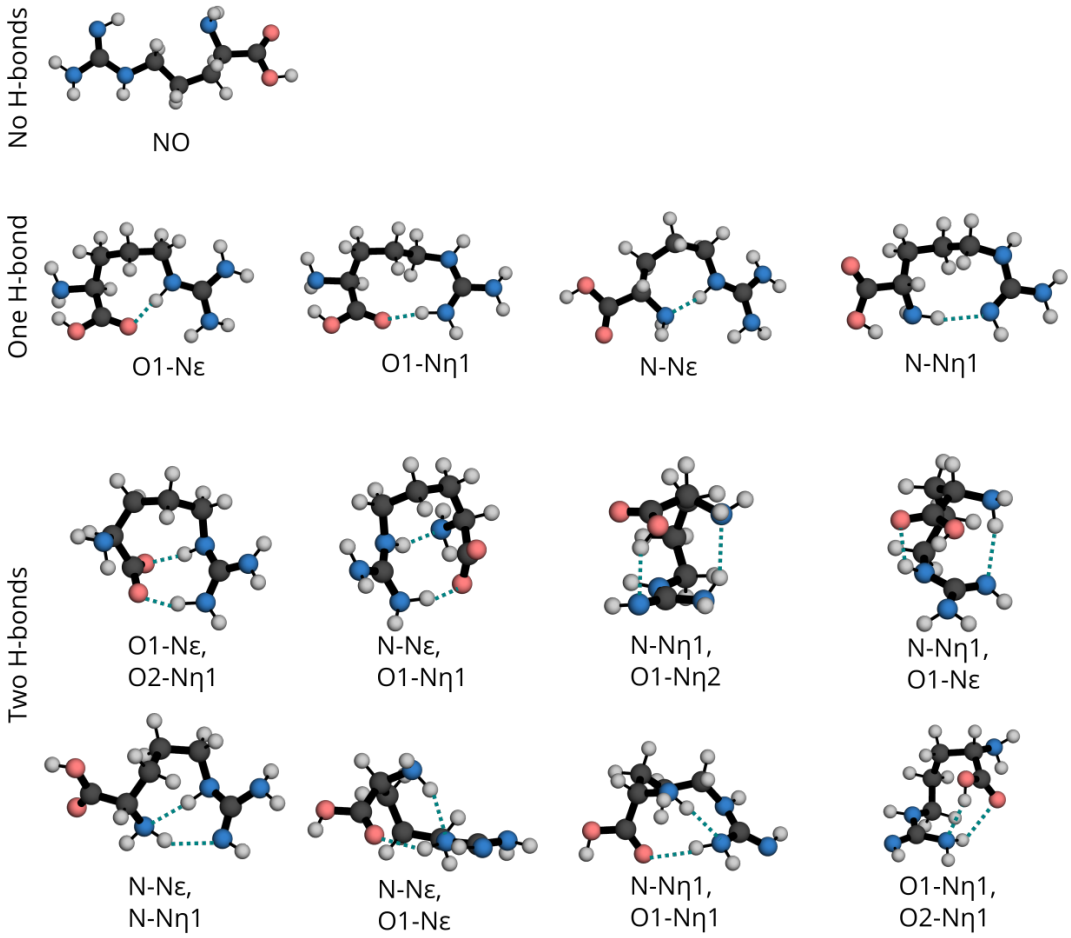

FIGURE S3 Labeling of all H-bond patterns considered in this manuscript.

3 | STRUCTURE SPACE REPRESENTATION

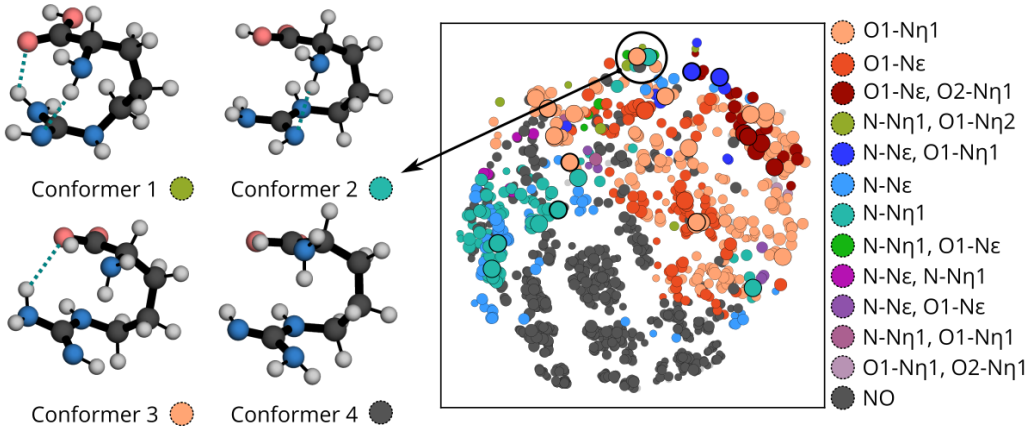

FIGURE S4 Representative conformers with similar backbone structure but different H-bonds within the molecule. The different H-bond pattern can cause energy differences of up to 0.2 eV for similar structures, as discussed in the main text.

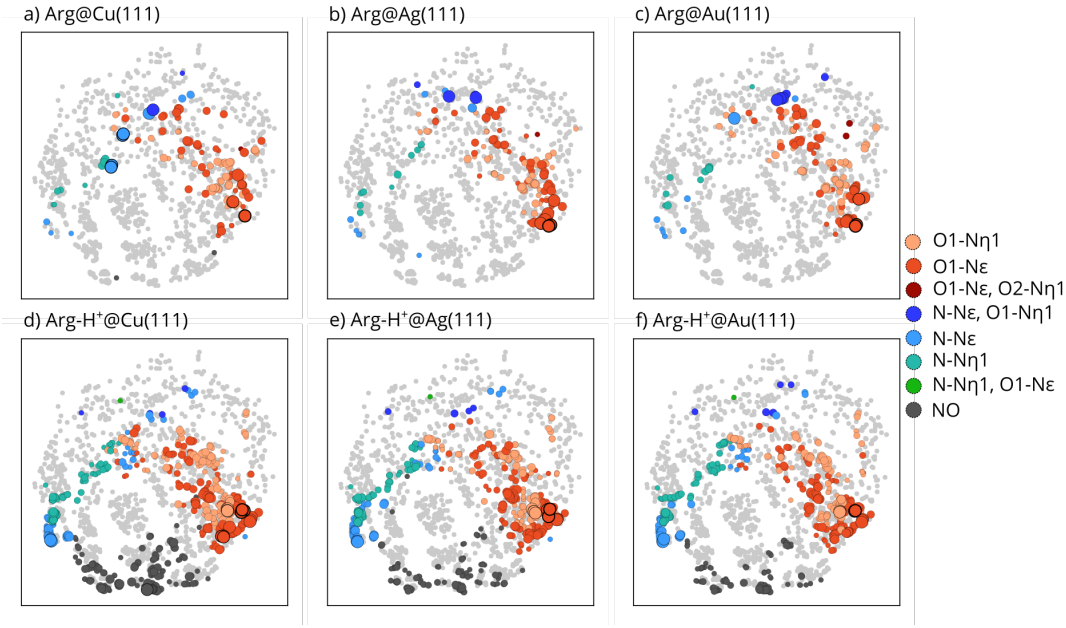

FIGURE S5 Projection of Arg and Arg-H^+ conformers adsorbed on the different metalic surfaces on the low-dimensional map of gas-phase Arg, colored according to the H-bond pattern.

TABLE S5 Number of different families within 0.1/0.5 eV energy range for different systems.

	Arg	Arg-H^+	Arg			Arg-H^+		
Atomnames			Cu	Ag	Au	Cu	Ag	Au
NO	0 /599	0/2	0/2	0/0	0/0	1 /162	0/124	0/98
N-Nε	0 /70	0/11	5/10	0/9	1/9	4 /80	3/79	3/77
N-Nη1	7 /87	0/20	0/11	0/12	0/13	0 /78	0/78	0/73
N-Nε, O1-Nη1	2 /11	2/4	1/2	2/6	4/6	0 /4	0/4	0/5
O1-Nε	2 /115	0/31	6/56	8/62	9/56	11/152	6/146	6/140
O1-Nη1	16/237	0/37	0/66	0/70	0/71	5 /135	4/115	5/109
O1-Nε, O1-Nη1	5 /27	0/2	0/1	0/1	0/2	0 /0	0/0	0/0
N-Nη1, O1-Nε	0 /5	0/1	0/0	0/0	0/0	0 /1	0/1	0/1
N-Nη1, O1-Nη1	0 /8	0/0	0/0	0/0	0/0	0 /0	0/0	0/0
N-Nε, N-Nη1	0 /8	0/0	0/0	0/0	0/0	0 /0	0/0	0/0
N-Nε, O1-Nε	0 /7	0/0	0/0	0/0	0/0	0 /0	0/0	0/0
N-Nη1, O1-Nη1	0 /2	0/0	0/0	0/0	0/0	0 /0	0/0	0/0
O1-Nη1, O2-Nη2	0 /3	0/0	0/0	0/0	0/0	0 /0	0/0	0/0

Regarding the SOAP kernels, we used 8 radial functions, 6 spherical functions, a 5.0 Åcutoff parameter, a Gaussian broadening of 0.5. We created all MDS plots with the `scikit-learn` package and the `sklearn.manifold.MDS` class. We used all default settings except for a pre-computed dissimilarity matrix (as explained in the main text) and 10 initializations (n_init=10).

4 | HARMONIC FREE ENERGIES

Free energies were calculated in the harmonic approximation [8, 9] for selected molecules adsorbed on surfaces within 0.1 eV range.

$$F(\mathrm{T}) = E_{\mathrm{PES}} + F_{\mathrm{vib}}(\mathrm{T}) + F_{\mathrm{rot}}(\mathrm{T}),$$

where E_{PES} is the total energy obtained with DFT (PBE+vdW$^{\mathrm{surf}}$ functional), and

$$F_{\mathrm{vib}}(\mathrm{T}) = \sum_{i}^{3N-6} \left[\frac{\hbar\omega_i}{2} + k_{\mathrm{B}} T \ln\left(1 - e^{-\beta\hbar\omega_i}\right) \right],$$

where N is the total number of atoms in the molecule (metal atoms were not displaced and were taken into account in external field), k_{B} is Boltzmann constant, T is the temperature, ω_i are vibrational frequencies obtained by diagonalization of Hessian matrix with use of developing version of phonopy-FHI-aims [10, 11] and

$$F_{\mathrm{rot}}(\mathrm{T}) = -k_{\mathrm{B}} T \ln\left[\frac{\sqrt{\pi}}{\sigma} \left(\frac{8\pi^2 I k_{\mathrm{B}} T}{h^2} \right) \right],$$

where I is the moment of inertia of the molecule obtained after diagonalization of the inertia tensor of the molecule. For the adsorbed conformers, rotational contributions are completely neglected since rotation around all principal axes of the molecule become internal vibrational modes of the system.

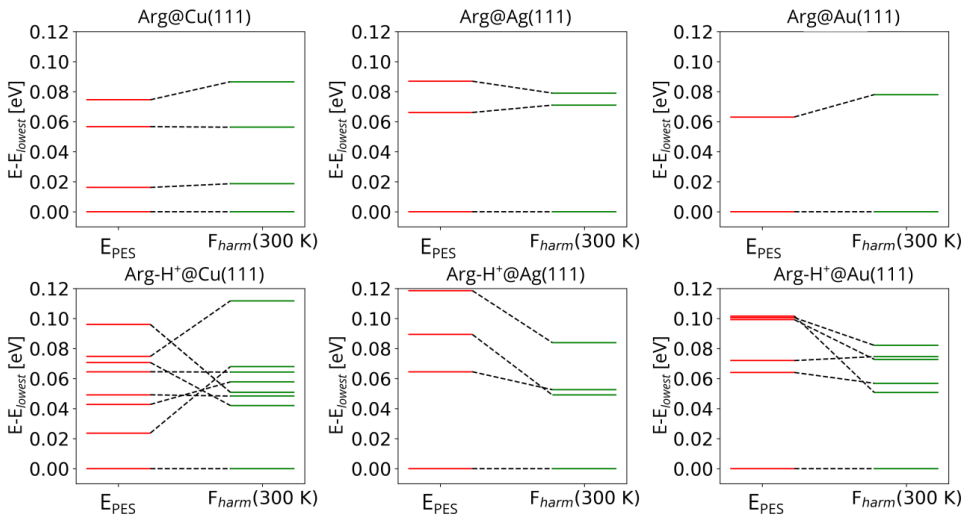

FIGURE S6 Harmonic free energies calculated for adsorbed structures within the lowest 0.1 eV total-energy range. $E_{\mathbf{PES}}$ corresponds to the total energy of the system obtained at DFT level and $F_{\mathbf{harm}}$ corresponds to the free energy of the system at 300 K calculated as described above.

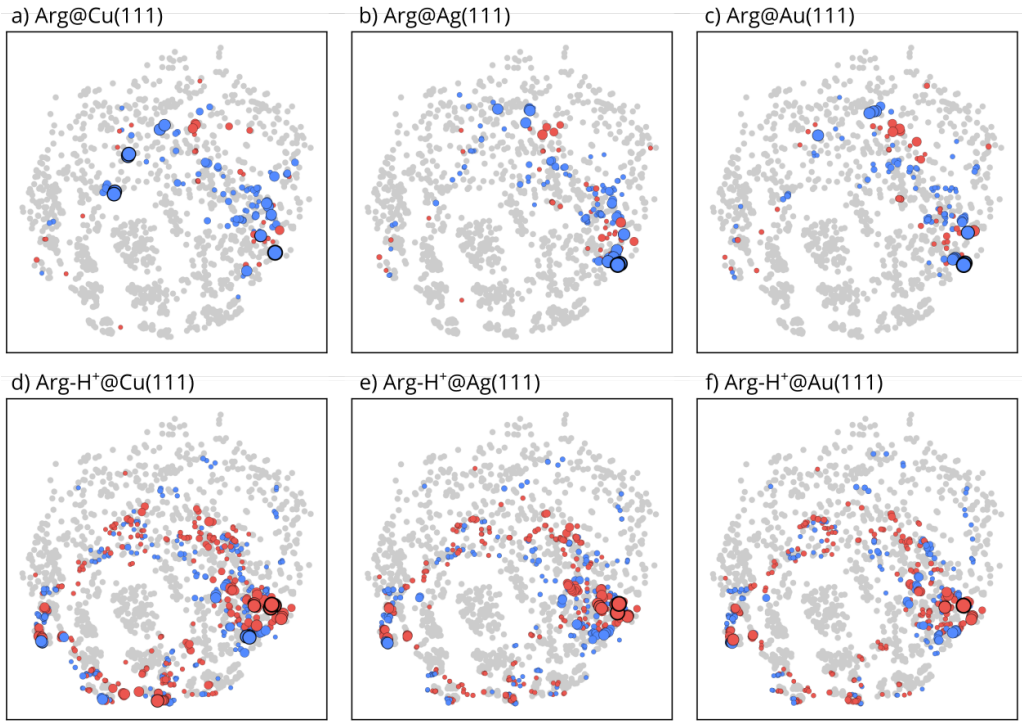

FIGURE S7 Low dimensional maps of Arg and Arg-H^+ adsorbed on Cu(111), Ag(111) and Au(111) color-coded with respect to the orientation of the $C_\alpha H$ group. Blue correspond to *up* orientation and red correspond to *down* orientation of the $C_\alpha H$ group.

5 | CHARGE REARRANGEMENT WHILE ON THE SURFACE

TABLE S6 Calculated charge on the molecule with use of Hirshfeld partial charge analysis and by integration of the electron density difference in the molecular region. Values are in electrons. Conformations are depicted in the following Figures S8-13.

Conformer	Hirshfeld	Integral	Conformer	Hirshfeld	Integral
Arg@Cu			Arg-H^+@Cu		
a	0.11	0.19	a	0.29	0.85
b	0.03	0.30	b	0.30	0.85
c	0.04	0.31	c	0.31	0.84
d	0.08	0.26	d	0.43	0.88
e	0.01	0.24	e	0.46	0.85
f	0.11	0.30	f	0.38	0.82
Arg@Ag			Arg-H^+@Ag		
a	0.04	0.15	a	0.28	0.83
b	-0.08	0.23	b	0.30	0.83
c	-0.03	0.24	c	0.31	0.82
d	-0.06	0.21	d	0.43	0.86
e	-0.13	0.16	e	0.46	0.85
f	0.05	0.14	f	0.36	0.86
Arg@Au			Arg-H^+@Au		
a	0.06	0.05	a	0.32	0.86
b	-0.01	0.29	b	0.29	0.86
c	0.00	0.30	c	0.34	0.85
d	-0.10	0.25	d	0.48	0.91
e	0.01	0.23	e	0.49	0.90
f	0.06	0.31	f	0.43	0.92

In order to take a look in electronic level alignments of interface system after adsorption the projected, angular-momentum resolved partial density of states (pDOS) averaged over all atoms of each species were calculated and normalized per molecule and per surface respectively. For corresponding isolated molecular geometry HOMO and LUMO levels were calculated and plotted together with interface pDOS. These calculations were performed with higher number of k-grid points: 6x6x1. Gaussian broadening was chosen to be 0.05.

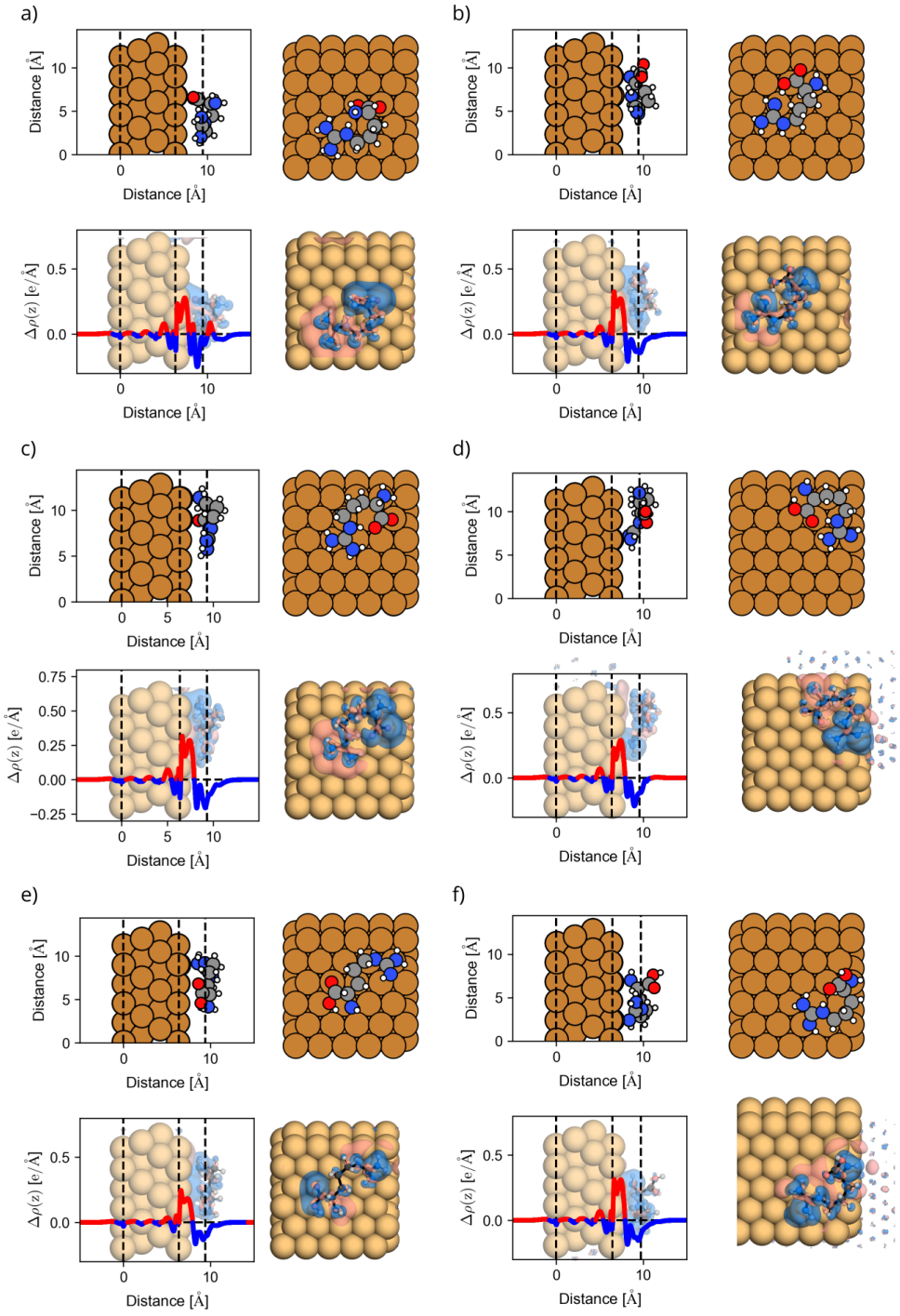

FIGURE S8 Side and top views of the adsorbed structures of Arg on Cu(111). Dashed black lines correspond to: average z position of the atoms in the lowest layer of the surface (left), average z position of atoms in the highest layer of the surface (middle), centre of the mass of the molecule (right). Red/blue solid lines (and also red/blue regions) correspond to the electron density accumulation/depletion, calculated as discussed in the manuscript in the section 2.3.

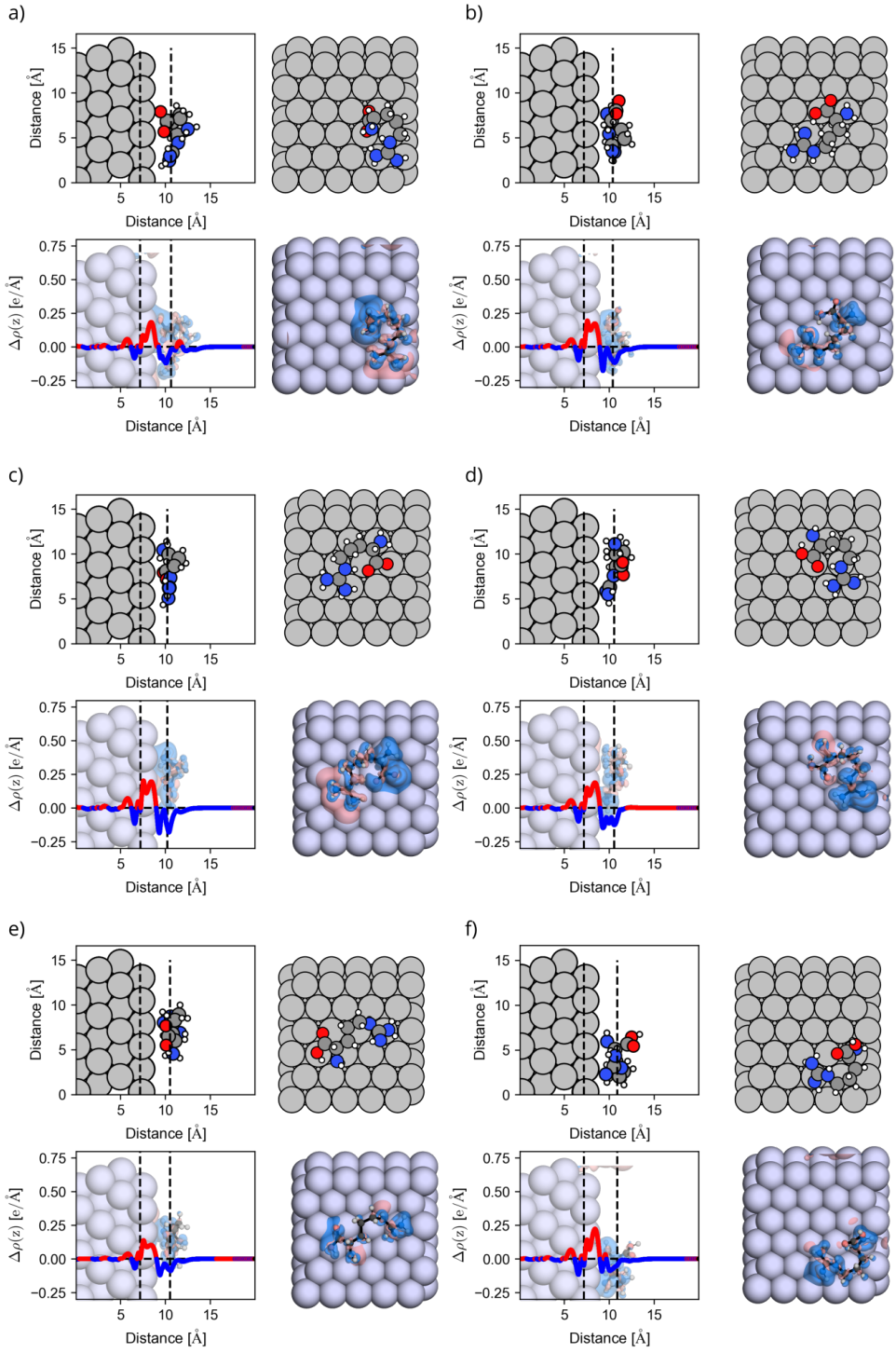

FIGURE S9 Side and top views of the adsorbed structures of Arg on Ag(111). Dashed black lines correspond to: average z position of the atoms in the lowest layer of the surface (left), average z position of atoms in the highest layer of the surface (middle), centre of the mass of the molecule (right). Red/blue solid lines (and also red/blue regions) correspond to the electron density accumulation/depletion, calculated as discussed in the manuscript in the section 2.3.

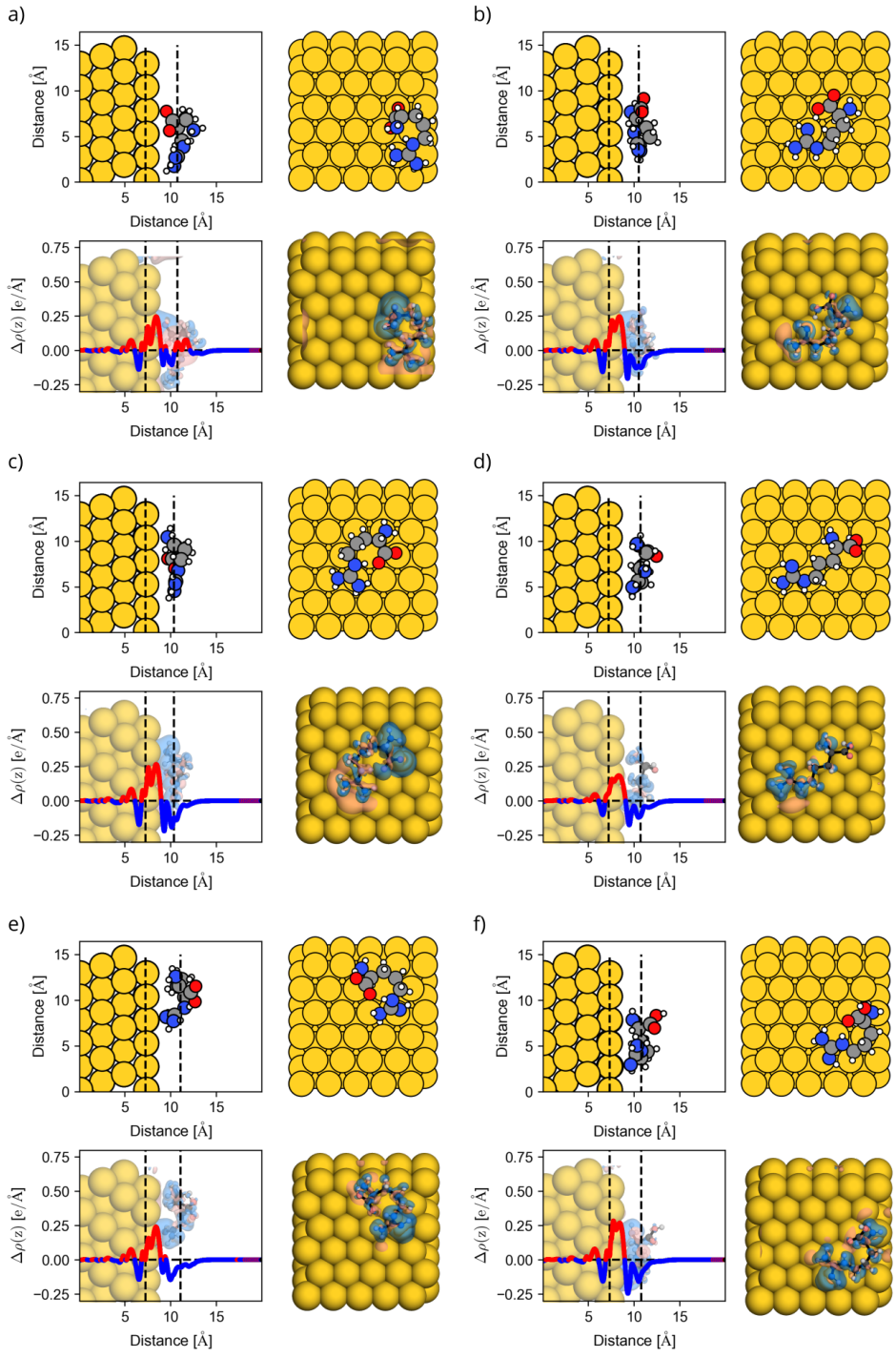

FIGURE S10 Side and top views of the adsorbed structures of Arg on Au(111). Dashed black lines correspond to: average z position of the atoms in the lowest layer of the surface (left), average z position of atoms in the highest layer of the surface (middle), centre of the mass of the molecule (right). Red/blue solid lines (and also red/blue regions) correspond to the electron density accumulation/depletion, calculated as discussed in the manuscript in the section 2.3.

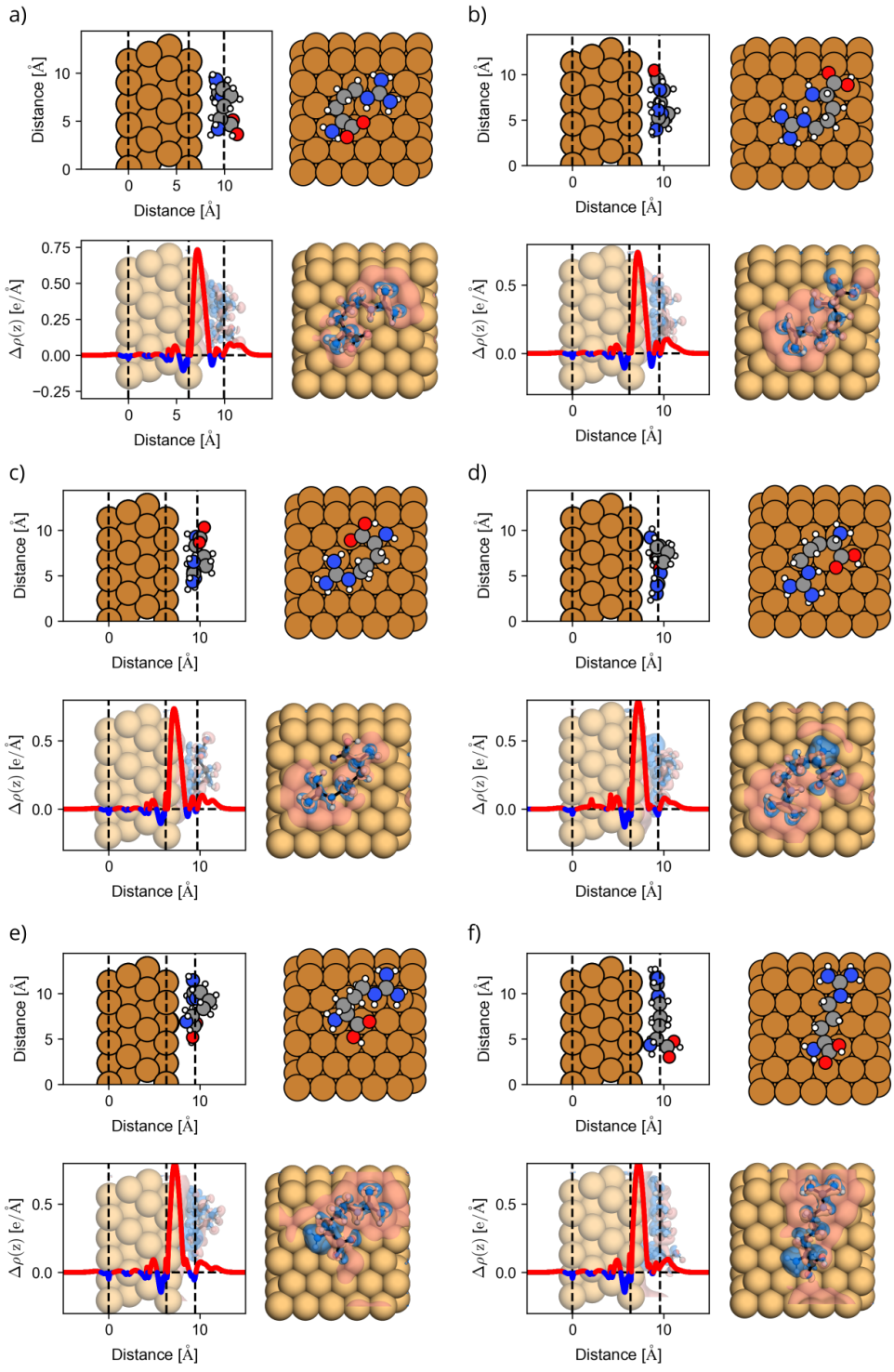

FIGURE S11 Side and top views of the adsorbed structures of Arg-H^+ on Cu(111). Dashed black lines correspond to: average z position of the atoms in the lowest layer of the surface (left), average z position of atoms in the highest layer of the surface (middle), centre of the mass of the molecule (right). Red/blue solid lines (and also red/blue regions) correspond to the electron density accumulation/depletion, calculated as discussed in the manuscript in the section 2.3.

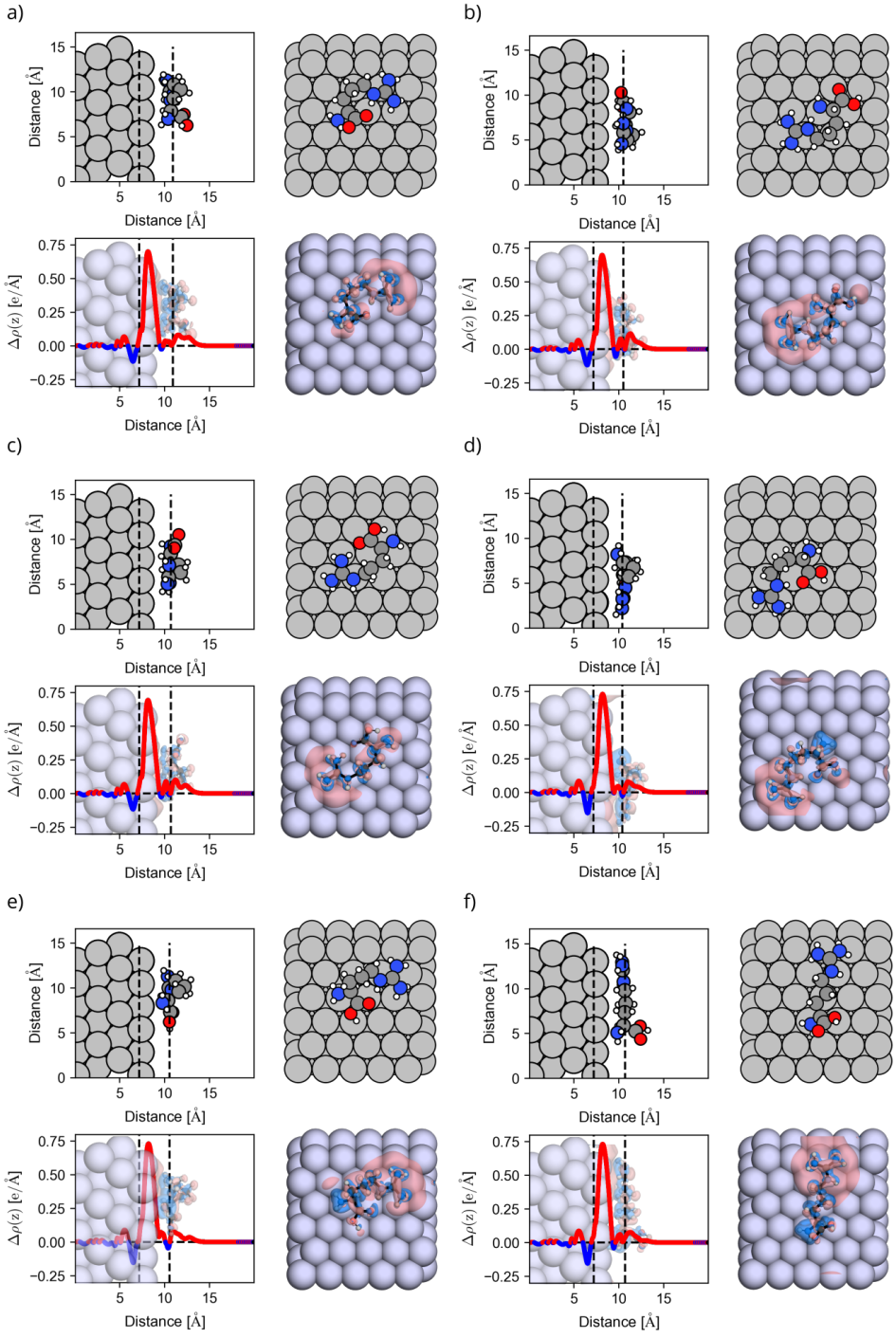

FIGURE S12 Side and top views of the adsorbed structures of Arg-H^+ on Ag(111). Dashed black lines correspond to: average z position of the atoms in the lowest layer of the surface (left), average z position of atoms in the highest layer of the surface (middle), centre of the mass of the molecule (right). Red/blue solid lines (and also red/blue regions) correspond to the electron density accumulation/depletion, calculated as discussed in the manuscript in the section 2.3.

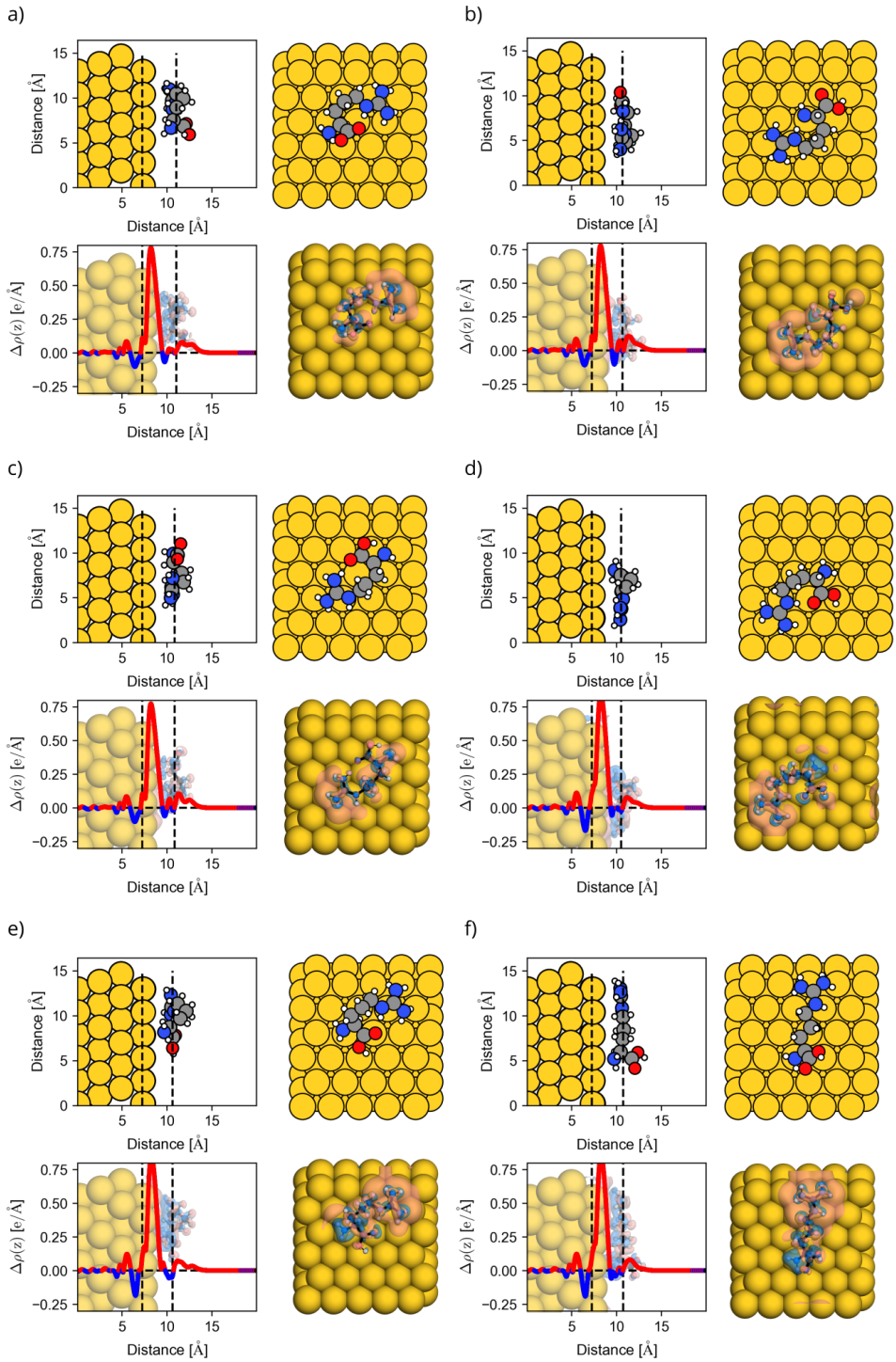

FIGURE S13 Side and top views of the adsorbed structures of Arg-H$^+$ on Au(111). Dashed black lines correspond to: average z position of the atoms in the lowest layer of the surface (left), average z position of atoms in the highest layer of the surface (middle), centre of the mass of the molecule (right). Red/blue solid lines (and also red/blue regions) correspond to the electron density accumulation/depletion, calculated as discussed in the manuscript in the section 2.3.

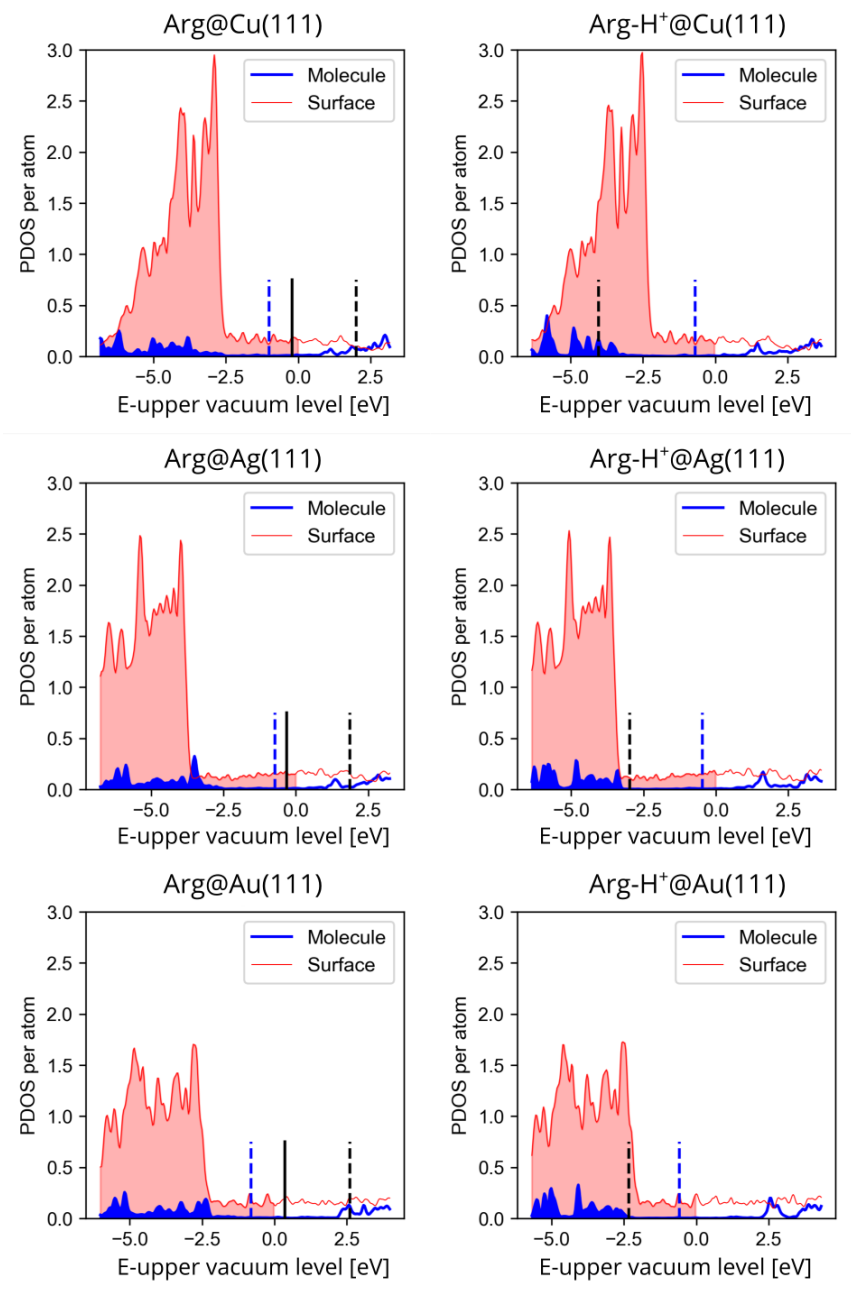

FIGURE S14 Projected densities of states of the lowest energy structures on each surface. Filled area corresponds to the occupied states below highest occupied state (VBM) of the whole system. HOMO (black solid line) and LUMO (black dashed line) are the states of the corresponding gas-phase molecular conformer calculated with the same geometry as it adopts when adsorbed. The Fermi energy of the pristine slab is depicted with blue dashed line.

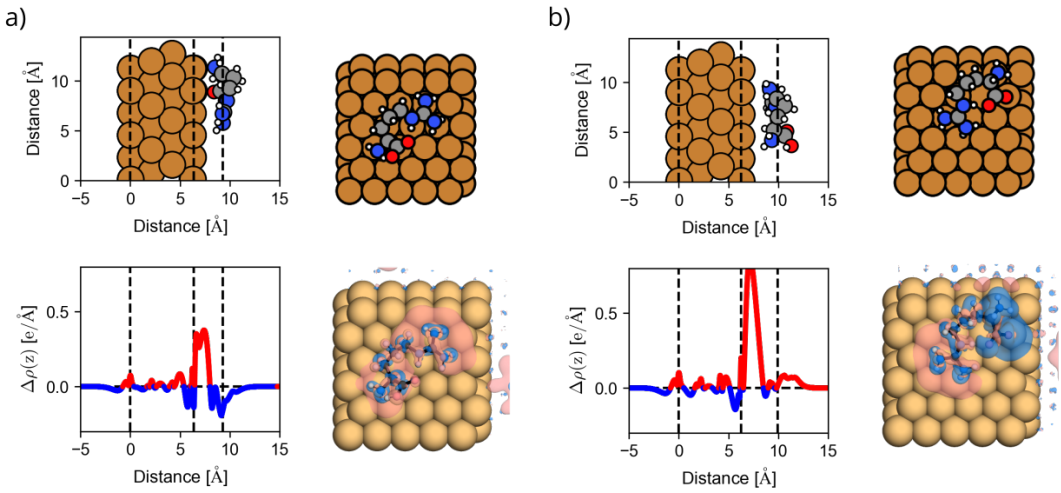

FIGURE S15 Side and top views of the adsorbed structures of a) Arg on Cu(111) (conformer c in Fig. S8) and b) Arg-H^+ on Cu(111) (conformer a in Fig. S11). Dashed black lines correspond to: average z position of the atoms in the lowest layer of the surface (left), average z position of atoms in the highest layer of the surface (middle), centre of the mass of the molecule (right). Red/blue solid lines (and also red/blue regions) correspond to the electron density accumulation/depletion, calculated as discussed in the manuscript in the section 2.3 with PBE0 functional.

6 | DEPROTONATION ON THE SURFACES

In Arg, we found it most favorable to detach the proton from the guanidino group, while for Arg-H^+, it was most favorable to detach the proton from the carboxyl group. In both cases we note that the final adsorbed species is a hydrogen, i.e., it does not carry a positive charge. We chose three representative conformers at each surface: the lowest energy structure and other two with different H-bonds within the molecule. We placed the detached proton at a distance of at least 2.5 Å from the molecule and fully optimized the dissociated structures. Comparing the energy difference between the final and initial states gives a lower limit for the dissociation barrier.

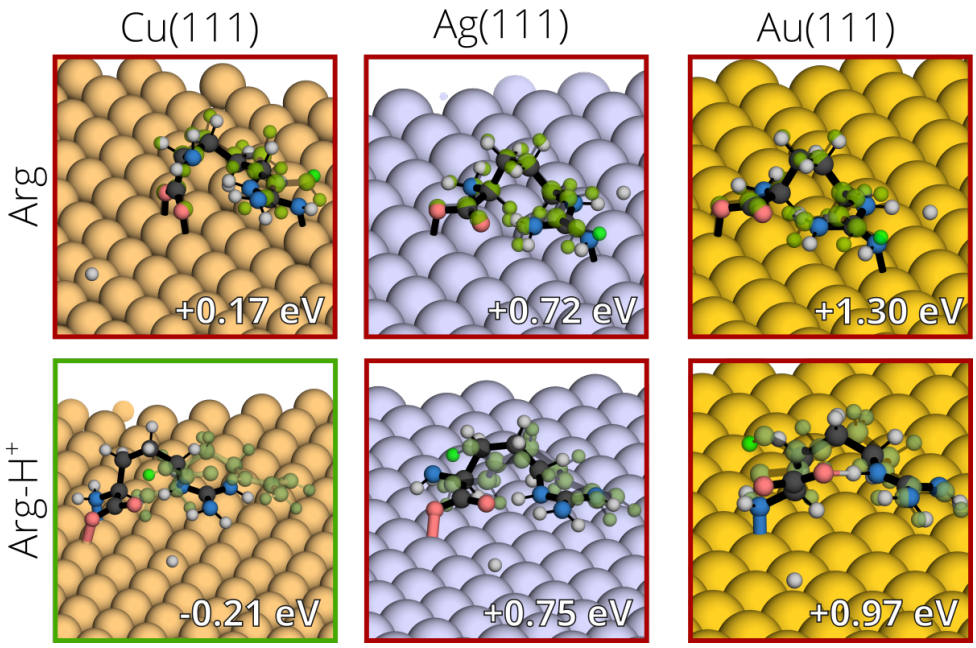

FIGURE S16 Representative structures that were analyzed for the calculation of the deprotonation energies. Colored structures represent the deprotonated relaxed structure. The green translucent structures represent the initial structure from which hydrogen was removed and placed on surface. The hydrogen that was removed is highlighted in bright green. ΔE (see main text) is also reported in each panel.

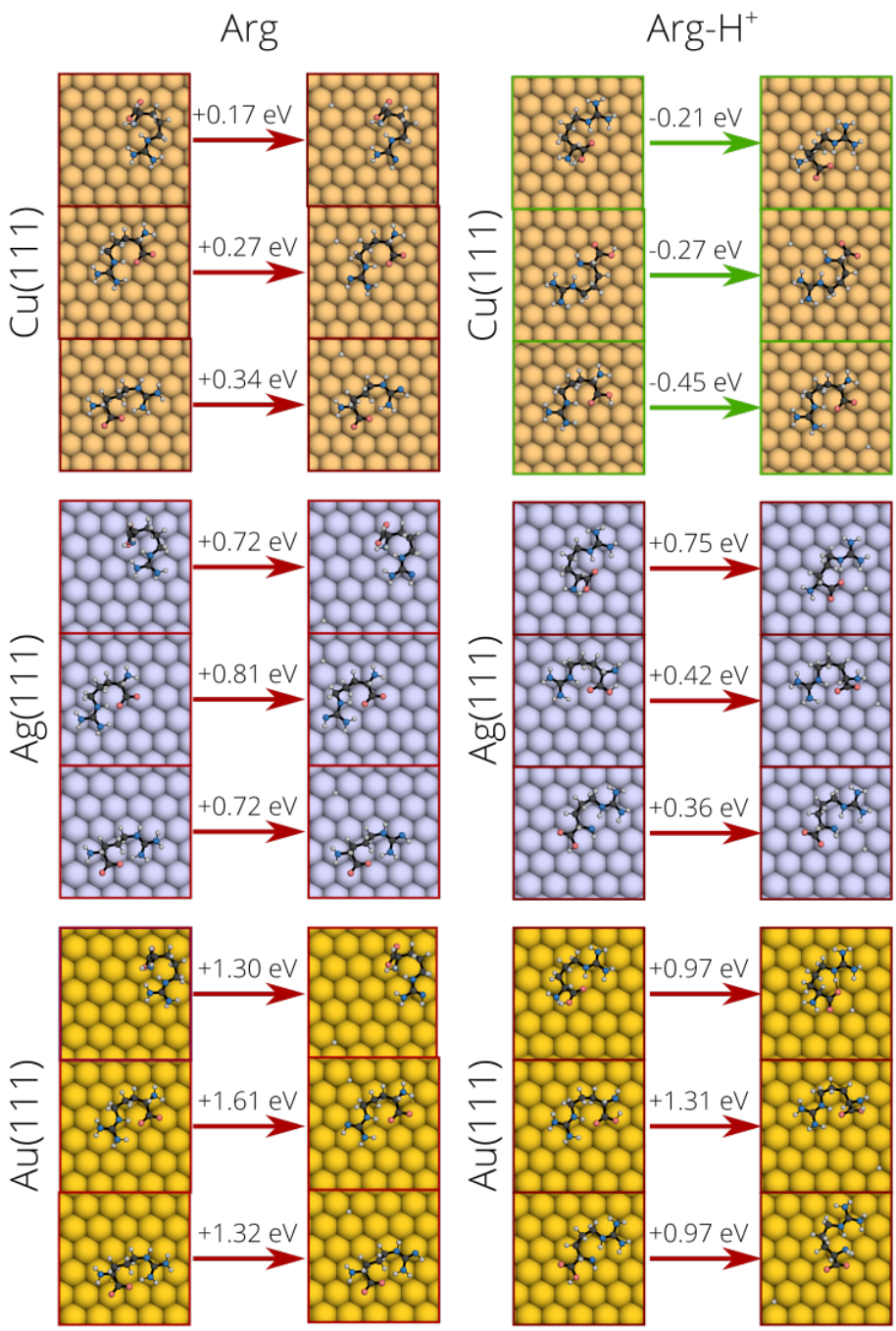

FIGURE S17 All structures that were analyzed for the calculation of the deprotonation energies. ΔE (see main text) is also reported in each panel.

7 | COMPARISON OF DFT WITH INTERFACE-FF

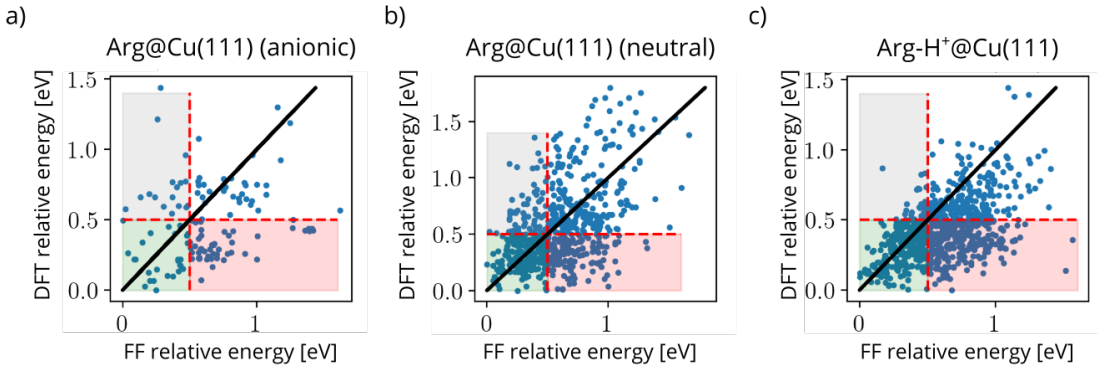

FIGURE S18 Comparison of the relative energies obtained from DFT optimized structures and the same structures after post-relaxation in with the INTERFACE force field. Dots on the diagonal line represent an optimal correlation. The red area marks structures that lie in the lower 0.5 eV energy range in DFT but above the 0.5 eV energy range in INTERFACE-FF. The green area marks the structures that are in the lower 0.5 eV energy range regardless of the level of theory. The grey area marks the structures that are above the 0.5 eV energy range in DFT but below the 0.5 eV energy range in INTERFACE-FF.

Selected local minima obtained at DFT level of theory were optimized with the INTERFACE-FF[12] using the NAMD package [13]. Calculations were performed with periodic boundary conditions with the same cell size and number of Cu atoms as in the DFT calculations. We obtained parameters for certain protonation states as described in the following. For the calculation of Arg, two protomers **P1** and **P3** (as denoted in the main text) had to be prepared. They are called "ARN" (P1) and "ARZ" (P3) in the topology file that is provided.

The parametrization of "ARZ" proceeded by taking the C-terminus in the deprotonated form (PRES CTER) and the N-terminus in the neutral form (PRES NNEU) from `top-all36-prot.rtf`, such that the protonation is COO-NH2 with total charge 0. The partial charge of the guanidino group is +1. Other parameters were taken from ARG (`top-all22-prot-metals.inp`) which is in the protonated form, by default, in CHARMM force field.

The parametrization of "ARN" proceeded by taking the parameters for neutral C-terminus and N-terminus (PRES CNEU and PRES NNEU from `top-all36-prot.rtf`) and the deprotonated methyl-guanidinium group (RESI MGU2) from `par-all36-cgenff.rtf`. Atom types and parameters for MGU2 were copied from `par-all36-cgenff.rtf`. The missing parameters related to joining MGU2 with the rest of Arg were manually added to the topology file. They were obtained from the corresponding values appearing in the protonated Arg, assuming that CG331 == CT2, NG311 == NC2, HGPAM1 == HC, NG2D1 == NC2, CG2N1 == C, where needed. The partial charge of CD atom was manually adjusted (decreased by 0.1) in order to have a neutral molecule with neutral guanidino group. Parameters for the neutral C-terminus and N-terminus were taken from the `top-all36-prot.rtf` file (PRES CNEU and PRES NNEU) and manually added to the customized file of topology.

ArgH named as "ARX" has total charge +1 (partial charge of guanidino group is also +1) and COOH-NH2 termini which is neutral. All the other parameters were directly taken from the INTERFACE-FF `all22-prot-metals` topology and parameter files.

We conclude from Fig. S18 that DFT (PBE+vdW^{surf}) and the INTERFACE-FF yield very different energy hier-

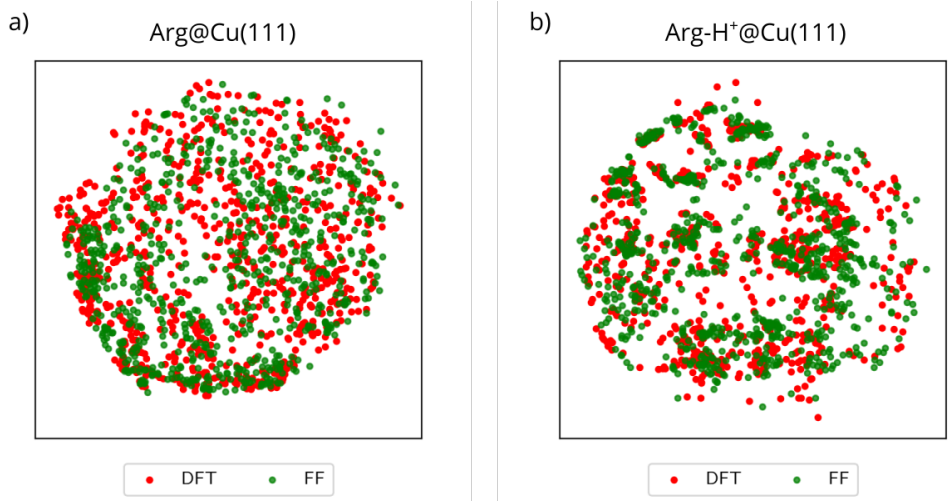

FIGURE S19 Low-dimensional map of the conformational space of the Arg and Arg-H^+ molecules adsorbed on the Cu(111) surface. The map was optimized considering all DFT and INTERFACE-FF structures. Green dots represent conformations obtained at DFT level of theory and red dots represent conformations obtained after geometry optimization with INTERFACE-FF. Close proximity of the dots reflects their structural similarity.

archies. However, from Fig. S19, we conclude that both levels of theory represent a similar conformational space. However, Table S7 shows that DFT and the FF yield different adsorption site preferences for the amino and carboxyl groups. In particular, DFT predicts that O will adsorb almost exclusively on top sites, consistent with the accepted adsorption site preference of CO groups on the pristine Cu(111) surface. The FF predicts a larger population of other adsorption sites, in particular hollow sites, compared to DFT.

TABLE S7 Surface site adsorption preferences of chosen chemical groups in Arg and Arg-H^+. All numbers are reported as a percentage of the total number of conformers optimized with DFT (PBE+vdW^{surf}) and the INTERFACE force field.

	Arg@Cu(111)				Arg-H^+@Cu(111)			
	Amino		Carboxyl		Amino		Carboxyl	
Adsorption site	DFT	FF	DFT	FF	DFT	FF	DFT	FF
Top	80	53	76	48	59	50	70	45
Bridge	9	18	14	18	18	20	15	22
Hollow-FCC	5	13	4	17	13	15	7	16
Hollow-HCP	6	16	5	17	10	15	9	18

references

[1] van Lenthe JH, Faas S, Snijders JG. Gradients in the ab initio scalar zeroth-order regular approximation (ZORA) approach. Chemical Physics Letters 2000;328(1):107–112.

[2] van Wüllen C. Molecular density functional calculations in the regular relativistic approximation: Method, application to coinage metal diatomics, hydrides, fluorides and chlorides, and comparison with first-order relativistic calculations. The Journal of Chemical Physics 1998;109(2):392–399.

[3] Perdew JP, Burke K, Ernzerhof M. Generalized Gradient Approximation Made Simple [Phys. Rev. Lett. 77, 3865 (1996)]. Physical Review Letters 1997;78(7):1396–1396.

[4] Liu W, Ruiz VG, Zhang GX, Santra B, Ren X, Scheffler M, et al. Structure and energetics of benzene adsorbed on transition-metal surfaces: density-functional theory with van der Waals interactions including collective substrate response. New Journal of Physics 2013;15(5):53046.

[5] Haas P, Tran F, Blaha P. Calculation of the lattice constant of solids with semilocal functionals. Phys Rev B 2009;79(8):85104.

[6] Tkatchenko A, Scheffler M. Accurate Molecular Van Der Waals Interactions from Ground-State Electron Density and Free-Atom Reference Data. Physical Review Letters 2009;102(7):073005.

[7] Ruiz VG, Liu W, Tkatchenko A. Density-functional theory with screened van der Waals interactions applied to atomic and molecular adsorbates on close-packed and non-close-packed surfaces. Physical Review B 2016;93(3):035118.

[8] McQuarrie DA. Statistical Mechanics. University Science Books; 2000.

[9] Fultz B. Vibrational thermodynamics of materials. Progress in Materials Science 2010;55(4):247–352.

[10] Togo A, Tanaka I. First principles phonon calculations in materials science. Scr Mater 2015;108:1–5.

[11] Fidanyan K, Development version of phonopy;. `https://github.com/fidanyan/phonopy`, accessed: 2019-03-01.

[12] Heinz H, Ramezani-Dakhel H. Simulations of inorganic–bioorganic interfaces to discover new materials: insights, comparisons to experiment, challenges, and opportunities. Chem Soc Rev 2016;45(2):412–448.

[13] Phillips JC, Braun R, Wang W, Gumbart J, Tajkhorshid E, Villa E, et al. Scalable molecular dynamics with NAMD. Journal of Computational Chemistry 2005;26(16):1781–1802.